Proc. of SPIE Vol. 1997, High Heat Flux Engineering II, ed. A M Khounsary (Nov 1993) Copyright SPIE

Infrared Missile Domes:

Heat Flux and Thermal Shock

Claude A. Klein
Raytheon Company, Research Division
131 Spring Street, Lexington, MA 02173
617-860-3113 (FAX-3195)

Abstract. Analytical expressions for the thermal shock resistance (TSR) of infrared (IR) missile domes involve a phenomenological stress factor that is not yet available but can be either extracted from the results of aerothermal shock testing or estimated on the basis of model-related considerations. The primary purpose of this contribution is to derive a simple formula for the allowable heat flux at the stagnation point, under conditions such that the boundary-layer flow remains laminar over the entire dome surface. Given the Hasselman parameter value of the dome material, it then becomes a straightforward matter to generate "laminar" Mach-altitude failure lines for thermally thin IR domes of specified diameter, wall thickness, and initial temperature. These failure lines are in essential agreement with the results of an independently performed finite-element analysis for domes made of alon, sapphire, and zinc sulfide, which validates the proposed model. Bearing in mind that, in a thermally thin regime, the TSR capability will be enhanced by making the dome as thin as possible, the model provides a direct measure of the ultimate TSR capability, in the sense that it yields the allowable stagnation temperature rise above the wall temperature, at the onset of the shock. With regard to contemplated dome-material candidates, an assessment based on U.S. Air Force requirements shows that, in addition to diamond, only two more candidates exhibit clearly superior TSR characteristics (GaP and Al_2O_3); small-diameter, highly truncated hemispherical domes made of GaAs, alon, or ZnS should be viable candidates for the medium-altitude application if a design safety factor of no more than two is acceptable.

Key Words. Aerothermal testing, analytical model, bending stress, infrared material, missile dome, performance assessment, stagnation temperature, thermal shock, thermal stress.

1. Introduction

The flight velocities of future-generation tactical missiles are projected to far exceed the performances of contemporary systems,[1] which raises the issue of how to assess the thermostructural capability of infrared (IR) dome material candidates. The sudden exposure to a supersonic flight environment subjects the dome to intense heat loads stemming from forced convection caused by the rise in temperature of the air in immediate contact with the outer dome surface. The dome's thermal response then results in temperature gradients through the thickness, which in turn generates transient stresses that may exceed the tensile strength of the dome material, thus causing "thermal shock" induced fracture. In a previous paper,[2] it was shown that the initial transient temperature distribution can be modeled quite effectively in the context of the "lumped parameter approximation," which has the advantage of providing some insight into the physical mechanisms that govern the thermal stresses of missile domes. The objective of that work was to reconsider the concept of a figure of merit for ranking potential dome materials from the point of view of their ability to withstand the thermal shock; in this connection, it was pointed out that an analytical expression for the thermal shock resistance (TSR) involves a phenomenological stress factor, which is not yet available but can be extracted from the results of aerothermal shock testing, as demonstrated elsewhere.[3] Here, I am relying on analytical/numerical techniques to derive and validate a simple formula for the allowable heat flux at the stagnation point of thermally thin domes, which should allow us to assess the TSR capability of IR domes in a fully laminar flow regime.

Any viable missile-dome structure (see Fig. 1) must be able to withstand both the mechanical stresses induced by aerodynamic pressure and the thermal stresses induced by aerodynamic heating. Because of the thermal expansion mismatch at the interface of the infrared dome and its support ring, it is generally accepted[4] that a "floating" attachment scheme that decouples the dome from the missile body will be required to ensure that the attachment does not inject stresses that may seriously affect the thermal shock performance. Furthermore, for truncated domes as in Fig. 1 ($\theta < 45$ deg), we may assume that laminar boundary-layer flow conditions prevail,[5] especially at higher flight altitudes ($Re < 3 \times 10^6$), which implies that the thermal shock environment, as defined by the Biot number, should be representative of a thermally thin regime ($Bi < 1$); as demonstrated in Ref. 2, this applies to most IR dome configurations/IR dome materials currently under consideration. These materials are listed in Table 1, which also includes relevant room-temperature properties as compiled by Harris.[6] This data set is believed to be quite adequate for our purposes, but it will be kept in mind that the fracture strength of optical ceramics is a very extrinsic property in the

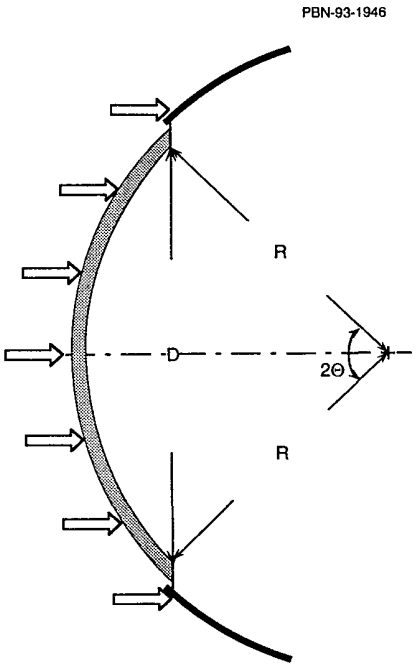

Fig. 1. *Generic infrared missile dome configuration.*

Table 1. *Infrared missile dome material candidates and their key properties*

Material candidate	Flexural strength (MPa)	Young's modulus (GPa)	Poisson's ratio	Thermal conductivity W/(m·K)	Thermal exp. coeff. ($10^{-6}K^{-1}$)
Al_2O_3	500	400	0.27	24	7
ALON	300	317	0.24	13	7
diamond	~2000	1050	0.16	2000	1
GaAs	60	86	0.31	53	6
GaP	100	103	0.31	97	6
MgF_2	100	115	0.30	12	10
spinel	180	280	0.26	15	7
Y_2O_3	150	170	0.30	14	7
ZnS	100	74	0.29	17	7
ZnSe	50	71	0.21	13	8

sense that it depends on microstructural features as well as the finish and the size of the test specimen. With regard to diamond, in particular, it should be noted that a flexural strength of *ca.* 2 GPa as given in Table 1 probably overestimates the true strength of chemically vapor deposited diamond since recent "ring-on-ring" measurements that were carried out on massive deposits point to characteristic strengths of no more than 250 MPa.

As mentioned earlier, the primary purpose of the present paper is to derive a simple formula for the allowable heat load at the stagnation point, under conditions such that the boundary-layer flow remains laminar over the entire dome surface (Sec. 2). In Sec. 3, I will demonstrate that this formula can be exploited to generate "Mach-altitude lines" that are in essential agreement with the results of a finite-element analysis of the transient stress.[7] And in Sec. 4, the formula will be used to assess the thermal shock performance of the dome material candidates listed in Table 1, which I will do in the context of realistic flight scenarios.[1] In this connection, it should be reiterated that the thickness of the dome plays a critical role in the sense that this parameter can have a major impact on the aerothermal stress.[2] I will address this issue in Sec. 4 with its implications in terms of the Biot number for domes of optimized thickness and the proper figure of merit for dome material candidates. Finally, the conclusions are stated in Sec. 5, while matters relating to the heat-transfer coefficient are presented in Appendix.

2. Allowable Stagnation Heat Flux

The initial transient temperature distribution generated by aerodynamic heating can be modeled in a simple manner, on using the "lumped parameter approximation" as in Ref. 2. If ΔT represents the surface temperature increase ($\Delta T = T_s - T_i$), and ΔX is the effective heat penetration depth, both at time t subsequent to the onset of convective heat transfer, the model yields

$$\Delta T \simeq (T_r - T_i)\sqrt{t/t_{th}} \quad , \tag{1}$$

where t_{th} is the thermal time constant,

$$t_{th} = \rho C_p k/h^2 \quad , \tag{2}$$

that controls the surface temperature increase (the notations are as specified in Table 2). Similarly, the lumped parameter approximation points to

$$\Delta X \simeq L\sqrt{t/t_d} \quad , \tag{3}$$

where t_d is the diffusion time constant,

$$t_d = \rho C_p L^2/k \ , \qquad (4)$$

which demonstrates that ΔX as well as ΔT increase as the square root of the elapsed time, but only for times t shorter than the two time constants. The ratio of the two time constants,

$$t_d/t_{th} = h^2L^2/k^2 = (Bi)^2 \ , \qquad (5)$$

immediately tells us that the dimensionless Biot number, *i.e.*, the ratio of bulk (L/k) and surface (1/h) resistances, best characterizes the transient heating process. For *thermally thick domes* ($Bi>1$), we have $t_d>t_{th}$, which implies that the surface temperature rise ΔT may approach the T_r-T_i limit at times t in the $t_{th}<t<t_d$ time "window," in other words, before the temperature of the backface begins to rise (see Fig. 2). For *thermally thin domes* ($Bi<1$), on the contrary, the backface will get hot long before the front reaches the recovery temperature, which implies that, according to Eq. (1), the peak temperature differential should be

$$(\Delta T)_p \simeq (T_r-T_i)\sqrt{t_d/t_{th}} = (T_r-T_i)\times Bi \qquad (6)$$

and, therefore, less than for "thick" domes.

In the absence of mechanical constraints (compliant mount!), aerodynamic heating will tend to produce tensile stresses on the inner (cold) surface of the dome and compressive stresses on the outer (hot) surface. At any angular station, the peak tensile stress that develops during the transient phase may then be expressed in a manner such as[8]

$$\sigma_p = (1/TSF)\alpha E'(\Delta T)_p \ , \qquad (7a)$$

where α is the thermal expansion coefficient, E' is the biaxial elastic modulus [$E'=E/(1-\nu)$], and $(\Delta T)_p$ refers to the peak temperature gradient across the wall; note that, in principle, the thermal stress factor (TSF) depends not only on the dome geometry and the attachment design but also on the temperature profile. Under laminar flow conditions, boundary-layer temperatures as well as heat-transfer coefficients are highest at the stagnation point, which implies that, in a thermally thin regime ($Bi<1$), the peak stress of concern should be approximately

$$\sigma_p \simeq \frac{1}{TSF}\times\frac{\alpha E}{1-\nu}\times Bi\times(T_{st}-T_{iw}) \qquad (7b)$$

based on Eq. (6) for the critical temperature difference.

Assume now that the failure stress relates to the nominal strength of the dome material through the fracture statistical factor FSF, *i.e.*,

$$(\sigma_p)_{lim} = \sigma_f/FSF \ . \qquad (8)$$

$$\Delta T = T_{ow} - T_{iw}$$

Thermally "Thick" (Bi ≥ 1)

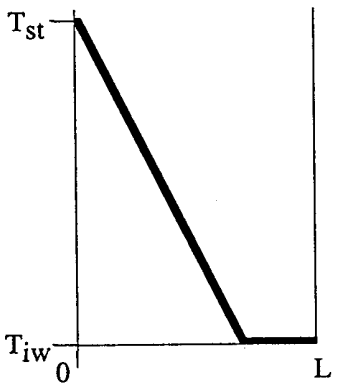

$$(\Delta T)_p \approx T_{st} - T_{iw}$$

Thermally "Thin" (Bi < 1)

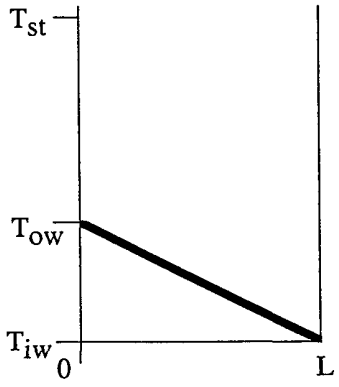

$$(\Delta T)_p \approx (T_{st} - T_{iw}) \times Bi$$

Fig. 2. *Schematic of the temperature profile through the dome thickness, under peak stress conditions (T_{iw}=inner wall temperature, T_{ow}=outer wall temperature, T_{st}=stagnation temperature).*

Table 2. *Glossary of symbols*

a	:	sound velocity in air	T	:	temperature, dome or air
Bi	:	Biot number	T_i	:	initial temperature
c_p	:	specific heat of air	T_r	:	recovery temperature
DSF	:	design safety factor	TSF	:	thermal stress factor
E	:	Young's modulus	TST	:	thermal shock temperature
E'	:	biaxial elastic modulus	u	:	air velocity
FoM	:	figure of merit	Z	:	flight altitude
FSF	:	fracture statistical factor	α	:	thermal expansion coefficient
h	:	heat-transfer coefficient	β	:	air velocity gradient
h'	:	h of 1-cm radius dome	γ	:	specific heat ratio
k	:	thermal conductivity	Δp	:	pressure differential
L	:	dome thickness	ΔT	:	temperature differential
L_{min}	:	recommended dome thickness	ΔX	:	heat penetration depth
M_∞	:	Mach number	μ	:	viscosity of air
p	:	air pressure	ν	:	Poisson's ratio
Pr	:	Prandtl number	ρ	:	density of air
Q	:	heat flux	ρC_p	:	heat capacity, dome material
R	:	dome radius	σ_f	:	nominal fracture strength
Re	:	Reynolds number	σ_{max}	:	maximum bending stress
R'_H	:	second Hasselman parameter	σ_p	:	peak thermal stress
St	:	Stanton number	*sub* iw	:	inner wall
t	:	elapsed time	*sub* st	:	stagnation point
t_d	:	diffusion time constant	*sub* ∞	:	free stream

The allowable stagnation temperature rise above the initial wall temperature then obeys the relation

$$(T_{st}-T_{iw})_{lim} \simeq \frac{TSF}{FSF}\times\frac{\sigma_f(1-\nu)}{\alpha E}\times\frac{1}{Bi} \ , \qquad (9)$$

which provides a direct measure of the TSR capability and emphasizes that the Biot number plays a key role in the process of assessing the stagnation temperature "jump" an IR dome can tolerate without undue risk of catastrophic failure. Since the appropriate Biot number is

$$Bi = h_{st}L/k \ , \qquad (10)$$

we now rewrite Eq. (9) as follows:

$$h_{st}(T_{st}-T_{iw})_{lim} \simeq \frac{TSF}{FSF}\times\frac{\sigma_f(1-\nu)k}{\alpha E}\times\frac{1}{L} \qquad (11)$$

and recall that, in the lumped parameter approximation, the product of heat-transfer coefficient and allowable temperature rise represents the allowable heat flux, *i.e.*, $h_{st}(T_{st}-T_{iw})_{lim} \equiv (Q_{st})_{lim}$. Furthermore, the material property combination on the right-hand side of Eq. (11) reproduces the well-known Hasselman parameter for thermally mild shocks, *i.e.*, $\sigma_f(1-\nu)k/(\alpha E) \equiv R'_H$. In this light, we conclude that, in a laminar flow environment, the allowable stagnation heat flux of thermally thin missile domes can be expressed in a remarkably compact form,

$$(Q_{st})_{lim} \simeq (TSF/FSF)(R'_H/L), \qquad (12)$$

which immediately tells us that the aerothermal performance will be impacted by the dome's thickness.

As formulated in Eq. (12), the theoretical expression for the heat-flux limit includes a numerical factor, TSF/FSF, that is not available for the complex situations of interest here; in the light of evidence presented elsewhere,[3] I am postulating that for modeling purposes the TSF/FSF ratio can be set equal to two, irrespective of dome material, dome configuration, and/or heat load. In effect, on assuming that the fracture statistical factor is essentially equal to one (1), in a thermal shock situation, this amounts to assigning a value of two (2) to the thermal stress factor, which should be acceptable because a spherical shell that is free to expand and has a linear temperature gradient across the thickness indeed exhibits peak stresses in accord with TSF=2.[9] In other words, for the purpose of establishing Mach-altitude limits for specified domes (see Sec. 3), or assessing the ultimate thermal shock resistance of dome material candidates as in Sec. 4, we may proceed on the assumption that TSF/FSF=2, *i.e.*, $(Q_{st})_{lim} = 2R'_H/L$, provides an acceptable measure of the allowable heat flux at the stagnation point of thermally thin domes, in a laminar flow regime.

3. Mach-Altitude Failure Lines

Under conditions as outlined above, that is, if the boundary-layer flow stays laminar over the entire dome surface, and the dome's response to transient heating is in the thermally thin mode, the Mach-altitude line that defines the "survival space" derives from the following statement:

$$h_{st}\left(T_{st}-T_{iw}\right)_{lim} = 2R'_H/L \ , \tag{13}$$

in accord with the conclusion of Sec. 2. We now recall[10] that the stagnation temperature depends on the flight altitude, through the free-steam temperature, as well as the Mach number, *i.e.*,

$$T_{st} = T_\infty(Z)\times\left(1+0.2M_\infty^2\right) \ . \tag{14}$$

Furthermore, the heat-transfer coefficient is best expressed in a manner such as

$$h_{st} = \frac{1.21J/(gK)}{\sqrt{R}}\sqrt{\rho_\infty\mu_\infty a_\infty}M_\infty\left(1+0.2M_\infty^2\right)^{0.1} \tag{15}$$

(see the Appendix), where ρ_∞, μ_∞, and a_∞ are functions of the altitude.[11] For the sake of convenience, I am introducing the functions f(Z) and $g(M_\infty)$,

$$f(Z) = \sqrt{\rho_\infty\mu_\infty a_\infty} \tag{16}$$

$$g\left(M_\infty\right) = 1+0.2M_\infty^2 \ , \tag{17}$$

which allows us to rewrite Eq. (13) in a manner most suitable for numerical processing:

$$f(Z)M_\infty\left[g(M_\infty)\right]^{0.1}\times\left[T_\infty(Z)g(M_\infty)-T_{iw}\right]=(1.65gK/J)R'_H\sqrt{R}/L \ . \tag{18}$$

Given the Hasselman parameter of the dome material, the radius and the thickness of the dome, plus the dome temperature at launch (or the onset of aerothermal loading), it is then straightforward to solve Eq. (18) in terms of the allowable Mach number at a specified flight altitude. Solutions to Eq. (18) thus provide the thermostructural boundary, or limit, where Mach number and flight altitude "combine" to produce stagnation-point heat loads of maximum tolerable intensity, *i.e.*, $(Q_{st})_{lim}$.

(U) The procedure is illustrated in Fig. 3, which displays "our" Mach-altitude lines (these are linear least-squares fit to numerical solutions) on plots generated by C. Resch by means of finite-element analysis (FEA) in conjunction with a temperature-dependent database.[7] The specifications (dome radius, thickness, initial wall temperature) are listed on top and apply

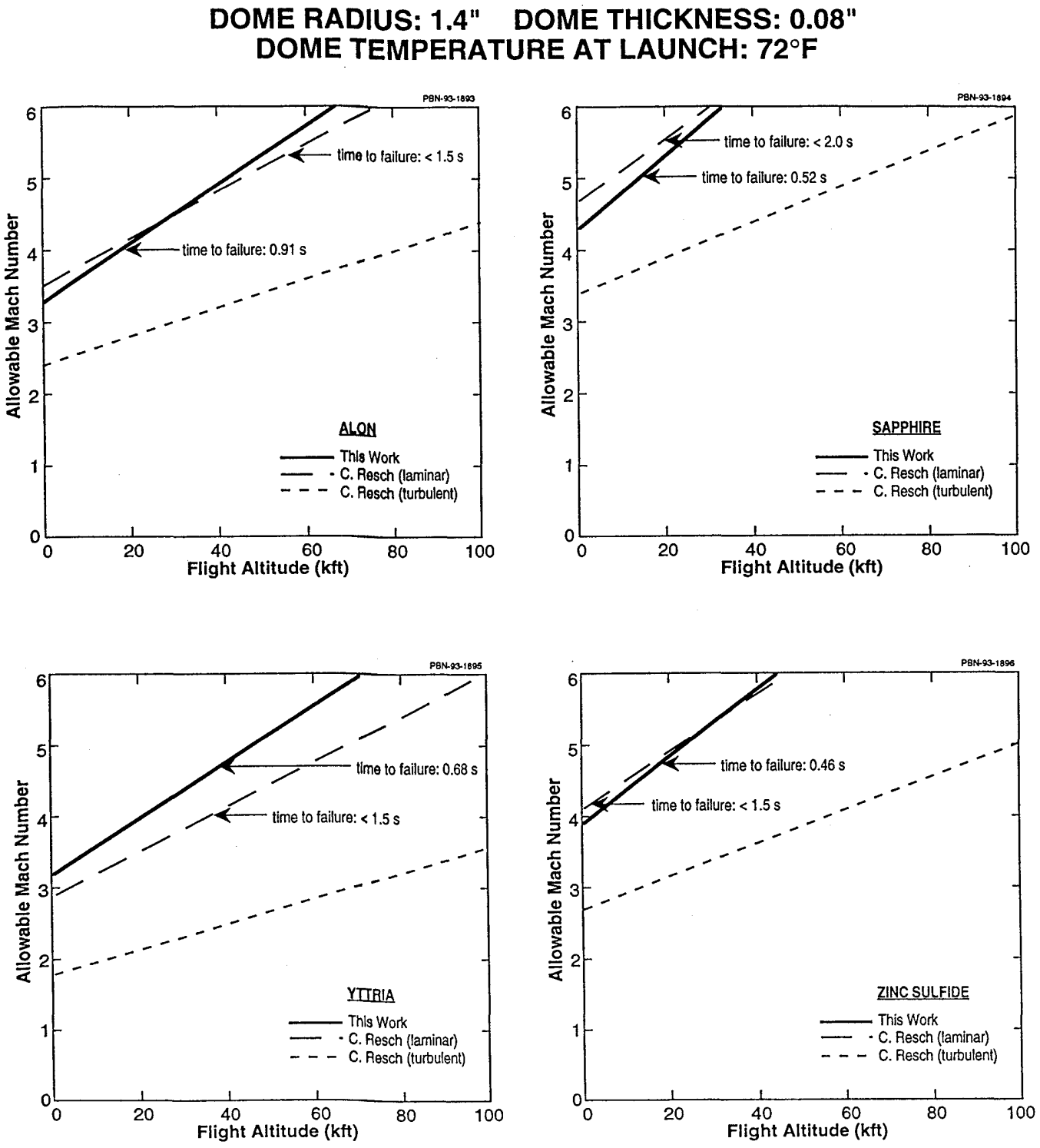

Fig. 3. *Mach-altitude failure lines for alon, sapphire, yttria, and zinc sulfide IR domes. The solid lines represent solutions to Eq. (18); the broken lines are as documented in Ref. 7.*

to domes made of alon, sapphire, yttria, and zinc sulfide; these domes have been assigned the same thickness (0.08 in.), which is inherently unrealistic because of enormous differences in fracture strength. In a laminar flow environment, they remain thermally thin, even at $M_\infty=6$, but this may not be true in a fully turbulent regime, in which case there is a dramatic decrease in thermal shock resistance (see Fig. 3). Three comments are in order. (a) The failure lines derived from Eq. (18) are in surprisingly good agreement with the "laminar" FEA results but for yttria; in this regard, I may point out that Resch assigns yttria a "maximum design stress" of 8 kpsi, which probably underestimates the allowable stress level since, according to Table 1, the nominal σ_f value is 150 MPa=21.75 kpsi. (b) Figure 3 also records the times at which failure is expected to occur under fully laminar flow conditions; our calculations,* which assume that the temperature gradient peaks just about when the inner-surface wall temperature begins to rise, that is, at times $t \simeq t_d$ (see Sec. 2), are in agreement with Resch's conclusion that the maximum stress peaks early into the flight. (c) Finally, we note that the finite-element analysis[7] disregards the attachment problem in the sense that "the structural model of the dome is unconstrained"; the agreement with solutions derived from Eq. (18) thus validates the TSF/FSF $\equiv 2$ *Ansatz*, but only for compliant attachments.

4. Thermal Shock Resistance Assessment

The thickness of the dome plays an essential role for two reasons: It may have an impact on the heat-flow pattern through the Biot number, and in a thermally thin regime (Bi<1), the thermal shock resistance will be enhanced by making the dome as thin as possible. Issues relating to minimum-thickness missile domes will be addressed in Sec. 4.1, while in Sec. 4.2, it will be shown how to express the Biot number for assessing the ultimate thermal shock resistance (Sec. 4.3). To illustrate the procedure, I propose to evaluate the TSR performance of candidate IR dome materials from the viewpoint of U.S. Air Force requirements[1] as delineated in Table 3; these requirements cover a wide range of altitudes and speeds (low-, medium-, and high-altitude scenarios), thus giving rise to a broad spectrum of aerostructural and aerothermal loads.

---

* Thermal conductivities are as listed in Table 1; heat capacities (ρC_p at room temperature) are as obtained from Ref. 12.

Table 3. *Air-to-air missile flight scenarios and relevant key numbers*

SCENARIO	LOW[a]	MEDIUM[a]	HIGH[a]
Flight altitude (km)	1	3	30
Mach number at launch	1	1.5	2
Mach number at speed	3	4	6
Free-stream pressure (psi)	13.0[b]	10.2[b]	0.174[b]
Stagnation pressure ratio	12.0	20.9	46.5
Pressure differential (psi)	143	203	7.91
Free-stream temperature (K)	282[b]	267[b]	227[b]
Stagnation temperature (K)	790	1121	1861
Heat-transfer coefficient ($Wcm^{-2}K^{-1}$)	0.324[c]	0.414[c]	0.081[c]

[a] See Ref. 1.
[b] Assumes a U. S. Standard Atmosphere.
[c] For a 1-cm radius dome.

4.1. Recommended Dome Thickness

The maximum bending stress of freely supported truncated hemispherical shells, that is, shells free to bend when subjected to the action of a uniform normal pressure, depends solely on the relative wall thickness and can be approximated by means of the relation[2]

$$\frac{\sigma_{max}}{\Delta p} \simeq \frac{0.581}{(L/R)^{3/2}} \qquad (19)$$

if Δp represents the pressure load. In supersonic flight, this load is less than, or equal to the differential pressure at the stagnation point,

$$\Delta p = p_\infty [(p_{st}/p_\infty) - 1] \ , \qquad (20)$$

where the ratio p_{st}/p_∞ refers to the pressure ratio across the aerodynamic shock, along the stagnation streamline.[10] In dealing with brittle materials, sound engineering practice dictates that the pressure-induced tensile stress shall not exceed a fraction of the nominal fracture strength, *i.e.*,

$$\sigma_{max} \leqslant \sigma_f/DSF \ , \qquad (21)$$

DSF representing the design safety factor ($2 \leqslant DSF \leqslant 4$, depending on the Weibull modulus of the dome material), which yields

$$\frac{L_{min}}{R} = 0.697(DSF)^{2/3}\left(\frac{\Delta p}{\sigma_f}\right)^{2/3} \qquad (22)$$

for the recommended dome thickness. The bar chart displayed in Fig. 4 summarizes our results for domes of 2.5-, 5-, and 10-cm radius made of the materials listed in Table 1; the safety factor was set equal to four (conservative design!) and the differential pressure equal to 1.40 MPa, which is indicative of peak pressure loads encountered on a medium-altitude trajectory (see Table 3).

4.2. Biot Number Evaluation

Since the heat-transfer coefficient varies inversely as the square root of the dome radius [see Eq. (15)], in other words, since

$$h_{st} = h'_{st}/\sqrt{R} \ , \qquad (23)$$

where h'_{st} refers to a 1-cm radius dome, it follows that the Biot number should be expressed in a manner such as

$$Bi^* = 0.697(DSF)^{2/3} \times h'_{st} (\Delta p)^{2/3} \times \frac{\sqrt{R}}{k(\sigma_f)^{2/3}} \qquad (24)$$

if the objective is to assess the ultimate TSR of an IR dome, in a laminar flow environment. This expression, which holds for a minimum-thickness dome, consists of a dimensionless numerical constant times the product of two factors: $h'_{st}(\Delta p)^{2/3}$ and $\sqrt{R}/(k\sigma_f^{2/3})$. The first factor involves only the Mach number and the flight altitude, hence reflects the severity of the aero environment; the second factor involves the dome radius in addition to key material properties (thermal conductivity and fracture strength). Figure 5 displays the results of evaluating Eq. (24) on the same basis as the thicknesses in Fig. 4, keeping in mind that the medium-altitude scenario is the most stressing in terms of pressure as well as heat load. With the exception of domes made of ZnSe, the response to instantaneous aerothermal heating will be in the "thin" mode, which disqualifies ZnSe as a potential IR dome material for advanced applications; of special interest is the case of diamond because its exceptionally low Biot number ($Bi^* < 0.001$) "explains" the outstanding TSR performance of this material.[13]

4.3. Thermal Shock Resistance

Returning now to Eq. (9) and setting the TSF/FSF ratio equal to two, we get

$$(T_{st} - T_{iw})_{lim} = 2 \times \frac{\sigma_f(1-\nu)}{\alpha E} \times \frac{1}{Bi} \qquad (25)$$

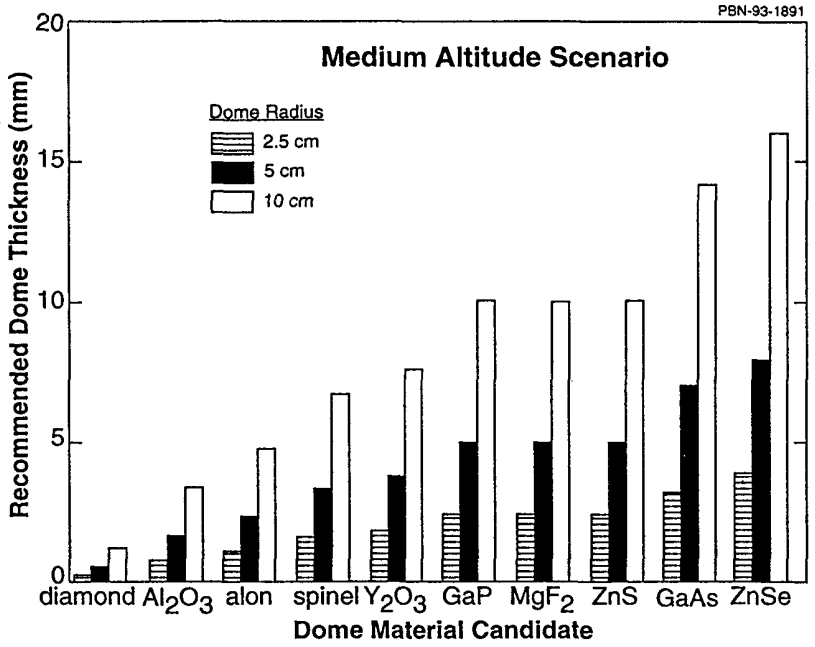

Fig. 4. *Required minimum thickness of IR missile domes on a medium-altitude trajectory; the safety factor was set equal to four.*

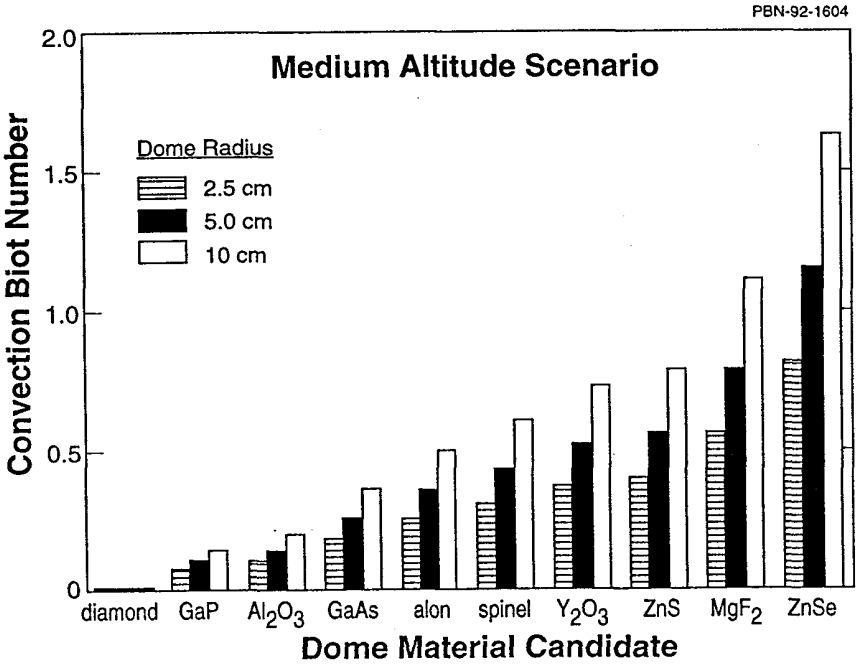

Fig. 5. *Laminar-flow convection Biot number of minimum-thickness IR missile domes on a medium-altitude trajectory; the safety factor was set equal to four.*

for the allowable recovery temperature rise above the initial wall temperature, which leads to

$$(T_{st}-T_{iw})^{*}_{lim} = \frac{2.87}{(DSF)^{2/3}} \times \frac{\sigma_f^{5/3}(1-\nu)k}{\alpha E} \times \frac{1}{h'_{st}(\Delta p)^{2/3}\sqrt{R}} \qquad (26)$$

for a thickness-optimized dome upon inserting the Biot number expression (24). At this point, we note that the material property combination that impacts the thermal shock performance is $\sigma_f^{5/3}(1-\nu)k/(\alpha E)$; the figure of merit for thermally thin IR dome material candidates,[2]

$$(FoM)_{Bi<1} = (\sigma_f)^{2/3} R'_H \ , \qquad (27)$$

thus emerges in a direct manner, which puts more weight on the fracture strength than the Hasselman parameter because of the role of σ_f in minimizing the thickness. Furthermore, Eq. (26) immediately suggests to measure the ultimate thermal shock resistance capability of an IR dome in a specified aero environment simply in terms of the allowable stagnation temperature rise when the safety factor is set equal to one (1); in other words,

$$TST \equiv (T_{st}-T_{iw})^{*}_{lim}(DSF)^{2/3} \ , \qquad (28)$$

where TST refers to the "thermal shock temperature," or maximum allowable temperature rise.

In this light, we conclude that, in a laminar flow/thermally thin environment, the thermal shock resistance capability is best quantified on the basis of

$$TST = \frac{2.87(FoM)_{Bi<1}}{h'_{st}(\Delta p)^{2/3}\sqrt{R}} \ , \qquad (29)$$

which emphasizes that it is the figure of merit $(FoM)_{Bi<1}$ that ranks the intrinsic capability of IR dome material candidates. The aero environment (Mach number and flight altitude) impacts the TSR performance through the normalized heat-transfer coefficient and the aerodynamic pressure load, exactly as anticipated considering the Bi # expression (24). The dome radius also plays a significant role since TST scales as $1/\sqrt{R}$, which demonstrates that, in fact, small-diameter domes are preferable, not only for achieving low drag but also for enhancing the thermal shock resistance, albeit this may conflict with considerations relating to optical resolution since apertures $D=2R\sin(\theta)$ of at least 2.5 cm are required in the infrared.[1]

The TST values of the nine remaining, thermally thin dome-material candidates are shown in Fig. 6, each bar chart referring to one of the three scenarios outlined in Table 3; as in Figs. 4 and 5, I am considering domes of 2.5-, 5-, and 10-cm radius. Survival or failure then

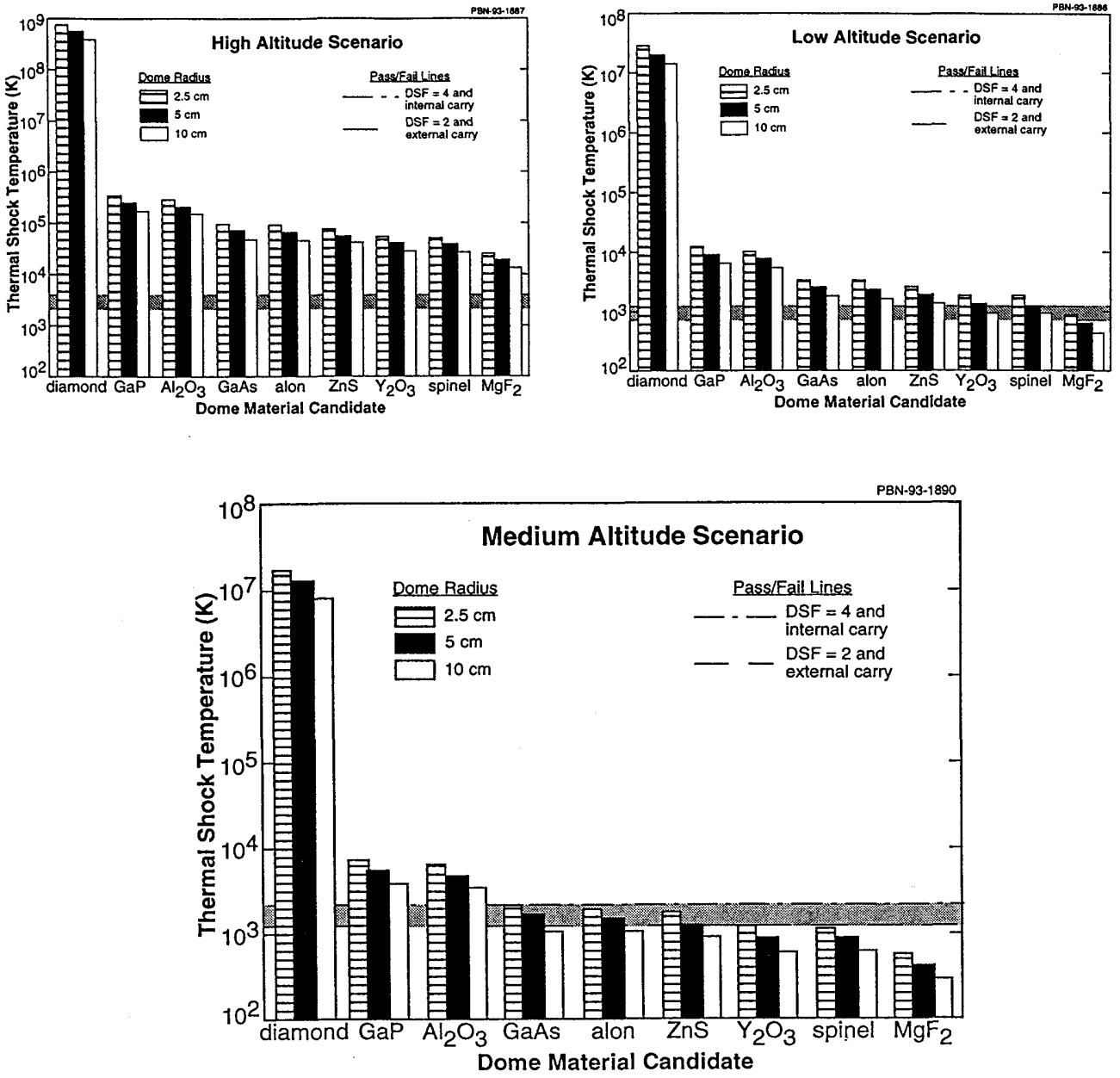

Fig. 6. *Thermal shock resistance capability of minimum-thickness missile domes on a low-altitude, a medium-altitude, and a high-altitude trajectory; the pass-fail lines reflect assumptions with regard to the design safety factor and the dome temperature at launch.*

simply reflects the conditions

$$(T_{st}-T_{iw})(DSF)^{2/3} < TST \qquad (30a)$$

and

$$(T_{st}-T_{iw})(DSF)^{2/3} > TST\ , \qquad (30b)$$

respectively, if T_{st} is the stagnation temperature on the contemplated trajectory, T_{iw} is the dome temperature at the onset of the shock, and DSF is the design safety factor. In Fig. 6, the two limiting "pass/fail lines" correspond to the more demanding case of DSF=4 in conjunction with internal carry (T_{iw}=293 K) and the less demanding case of DSF=2 in conjunction with external carry [$T_{iw}=(T_{st})_o$]; they demonstrate that, from a thermal shock point of view, and independently of considerations relating to tolerable steady-state temperatures, the following can be said about IR dome material candidates. (a) There are three obviously superior candidates (sapphire, gallium phosphide, and diamond), diamond providing by far the highest level of capability, perhaps as much as three orders of magnitude if the fracture strength is as listed in Table 1. (b) Gallium arsenide, alon, and zinc sulfide show surprisingly little variation in TSR capability and should be acceptable for the medium-altitude application if the dome diameter does not exceed 4 in. (c) Based on property values as given in Table 1, it is seen that magnesium fluoride, spinel, and yttria are relatively poor performers, even on a low-altitude/Mach-3 trajectory, but appear to be suitable for duties restricted to very high altitudes.

5. Conclusion

Under laminar flow conditions, the thermal shock performance of an unconstrained, thermally thin IR missile dome is controlled by the allowable heat flux at the stagnation point: $(Q_{st})_{lim} = (TSF/FSF)R'_H/L$, where TSF/FSF represents an *ad hoc* phenomenological factor, R'_H refers to the second Hasselman parameter, and L designates the dome thickness. Elementary considerations relating to the fracture statistical factor ($FSF \geq 1$) and the thermal stress factor ($TSF \geq 2$) suggest TSF/FSF ratios of approximately two (~2), in accord with some experimental evidence discussed elsewhere.[3] In the absence of additional information, I am postulating that setting the stress factor ratio equal to two (TSF/FSF ≡ 2) should be appropriate for modeling purposes, irrespective of dome material, aspect ratio, and heat load.

In this framework, and given the Hasselman parameter values, it becomes a straightforward matter to derive the "laminar" Mach-altitude failure lines for IR domes of specified diameter, wall thickness, and initial temperature (see Fig. 3). These failure lines are in surprising agreement with the results of an independently performed finite-element analysis[7] for domes made of alon, sapphire, and zinc sulfide, which validates the *Ansatz* $(Q_{st})_{lim} = 2R'_H/L$. Furthermore, in the context of interest here, laminar failure occurs shortly ($\lesssim$ 1 s) after the onset of aerothermal exposure, again in agreement with FEA results, which substantiates using the lumped parameter approximation to describe the heat-flow pattern.

In a thermally thin regime (Bi<1), the thermal shock resistance capability will be enhanced by making the dome as thin as possible, which suggests that, for the purpose of assessing the ultimate TSR of an IR dome, the Biot number should be expressed as in Eq. (24). This procedure provides a direct measure of the TSR capability in the sense that it yields the allowable stagnation temperature rise above the wall temperature at the onset of the shock, which demonstrates that the appropriate material figure of merit is indeed $(\sigma_f)^{2/3}R'_H$ as advocated in Ref. 2. With regard to contemplated dome material candidates, an assessment of their TSR capability based on U.S. Air Force requirements shows that, in addition to diamond, there are only two more candidates with clearly superior characteristics (GaP and Al_2O_3), but small-diameter GaAs, alon, and ZnS domes should be acceptable for the medium-altitude application on the condition that the boundary-layer flow remains laminar over the entire dome surface.

6. Acknowledgment

I wish to thank Cheryl Resch, Johns Hopkins Applied Physics Laboratory, for providing a copy of Ref. 7 and for granting permission to reproduce her results.

Appendix: Practical Formula for the Heat-Transfer Coefficient

In the framework of conventional boundary-layer theory, heat-transfer coefficients are best evaluated by introducing a dimensionless expression called the Stanton number, which relates the heat-transfer coefficient to "local" flow parameters[14]:

$$h = (St)\rho c_p u \ . \qquad (A-1)$$

In a laminar flow situation, the Stanton number at any point on a sphere can be expressed as follows[15]:

$$St = 0.763(Pr)^{-0.6} \times (Re)^{-0.5} \times \sqrt{\beta(x/u)} \qquad (A-2)$$

if x measures the length of boundary-layer run from the stagnation point. In addition to the numerical constant, this expression is made up of three dimensionless factors that involve (a) the fluid properties as specified by the Prandtl number,

$$Pr = \mu c_p/k \ , \qquad (A-3)$$

(b) the flow conditions as characterized by the local Reynolds number,

$$Re = \rho u x/\mu \ , \qquad (A-4)$$

and (c) the velocity gradient at the outer edge of the boundary layer,

$$\beta = (\partial u/\partial x)_x \ . \qquad (A-5)$$

At the stagnation point, this velocity gradient is[14]

$$\beta_{st} = \sqrt{8\left(\rho_\infty/\rho_{st}\right)} \times \left(u_\infty/2R\right) \quad , \qquad \text{(A-6)}$$

where R designates the radius of curvature of the outer wall. Furthermore, we may assume that the Prandtl number will be equal to about 0.70, at "supersonic" stagnation temperatures.[16] It then becomes straightforward to express the stagnation heat-transfer coefficient in a manner such as

$$h_{st} \simeq 1.6\left(c_p/\sqrt{2R}\right) \times \sqrt{\rho_\infty \mu_\infty u_\infty} \times \left(\rho_{st}/\rho_\infty\right)^{1/4} \times \sqrt{\mu_{st}/\mu_\infty} \quad , \qquad \text{(A-7)}$$

which lends itself to further reduction on using classical results of compressible fluid dynamics.

Equation (A-7) includes the stagnation-point density and the stagnation-point viscosity, both measured relative to free-stream values. In this regard, we note that the density ratio is[10]

$$\frac{\rho_{st}}{\rho_\infty} = \left[\frac{(\gamma+1)M_\infty^2}{(\gamma-1)M_\infty^2+2}\right]\left[1+\frac{\gamma-1}{2} \times \frac{(\gamma-1)M_\infty^2+2}{2\gamma M_\infty^2-(\gamma-1)}\right]^{\frac{1}{\gamma-1}} \quad , \qquad \text{(A-8a)}$$

where γ refers to the specific heat ratio of air (γ=1.4), and can be approximated as follows:

$$\frac{\rho_{st}}{\rho_\infty} \simeq \frac{1.3M_\infty^2}{1+0.2M_\infty^2} \quad . \qquad \text{(A-8b)}$$

The viscosity ratio can be obtained directly from the temperature ratio on the basis of the empirical relation[17]

$$\mu_{st}/\mu_\infty \simeq \left(T_{st}/T_\infty\right)^{0.7} \quad , \qquad \text{(A-9a)}$$

which holds at temperatures encountered in supersonic flight and leads immediately to

$$\mu_{st}/\mu_\infty \simeq \left(1+0.2M_\infty^2\right)^{0.7} \qquad \text{(A-9b)}$$

since the stagnation temperature relates to the free-stream temperature through Eq. (14).

Returning now to Eq. (A-7), and upon inserting the ratios (A-8b) and (A-9b), we find that the heat-transfer coefficient at the stagnation point can be approximated in a fairly simple manner:

$$h_{st} \simeq 1.7\left(c_p/\sqrt{2R}\right) \times \sqrt{\rho_\infty \mu_\infty a_\infty} \times M_\infty \left(1+0.2M_\infty^2\right)^{0.1} \quad , \qquad \text{(A-10)}$$

which indeed yields Eq. (15) considering that the specific heat of air at constant pressure is 0.24 cal/(gK). This equation characterizes the aerothermal heat transfer at the stagnation point of a

hemispherical dome in terms of readily available parameters: the properties of the atmosphere, the flight Mach number, and the radius of the dome. In this connection, we note that (a) the coefficient h_{st} scales as the reciprocal square root of the radius and, therefore, implies higher heating rates for smaller diameter domes; (b) altitude has a very significant effect, mainly because h_{st} varies as the square root of the air density; and (c) the formula gives results that are in satisfactory agreement with predictions based upon more elaborate methods of evaluating laminar heat-transfer coefficients.[18]

References

1. J. Rowe, A. Blume, and E. Boudreaux, "Dual-Mode Dome Requirements for Future Air-to-Air Missiles," *Proceedings of the Third DoD Electromagnetic Windows Symposium* (IIT Research Institute, Chicago/IL, 1989), pp. 79-95.
2. C. Klein, "Infrared Missile Domes: Is there a Figure of Merit for Thermal Shock?" *SPIE Proceedings*, vol. 1739 (1992), pp. 230-53.
3. C. Klein, "Thermal Shock Resistance of Infrared Missile Domes: Analysis and Testing (U)," *Proceedings of the Fifth DoD Electromagnetic Windows Symposium* (Wright Laboratory, WPAFB/OH, 1993), in print.
4. C. Lee, "Evaluation of Several IR/RF Dome Configurations Subjected to High-Speed Flight Environments," *Proceedings of the Fourth DoD Electromagnetic Windows Symposium* (Office of Naval Technology, Arlington/VA, 1991), pp. 24-32.
5. I. Beckwith and J. Gallagher, "Heat Transfer and Recovery Temperatures on a Sphere with Laminar, Transitional, and Turbulent Boundary Layers at Mach Numbers of 2.00 and 4.15," *Document No. T.N. 4125* (National Advisory Committee for Aeronautics, Washington/DC, 1957), 59 pp.
6. D. Harris, "Powder Processing Technology for GaAs and GaP Infrared-Transmitting Materials," *Document No. NWC-TP-7145* (Naval Weapons Center, China Lake/CA, 1991), 24 pp.
7. C. Resch, "Structural Limits of Sapphire, Zinc Sulfide, ALON, and Yttria IR Domes Based on Altitude and Mach Number," *Document No. AM-89-E0077* (Applied Physics Laboratory, Laurel/MD, 1989), 24 pp.
8. F. McClintock, ed., "Mechanical Properties of Infrared Transmitting Materials," *Document No. NMAB-386* (National Academy of Sciences, Washington/DC, 1978), 293 pp.
9. S. Timoshenko and W. Woinowsky-Krieger, *Theory of Plates and Shells* (McGraw-Hill Book Co., New York/NY, 1959), chap. 16.
10. A. Shapiro, *The Dynamics and Thermodynamics of Compressible Fluid Flow* (The Ronald Press Co., New York/NY, 1953), vol. 1.
11. M. Harris, "Meteorological Information," in *American Institute of Physics Handbook* (McGraw-Hill Book Co., New York/NY, 1972), chap. 2k.
12. J. Browder, S. Ballard, and P. Klocek, "Physical Properties of Crystalline Infrared Optical Materials," in *Handbook of Infrared Optical Materials* (Marcel Dekker Inc., New York/NY, 1991), chap. 6.
13. C. Klein, "Diamond Domes for High-Velocity Missiles: An Initial Assessment," *Proceedings of the Fourth DoD Electromagnetic Windows Symposium* (Office of Naval Technology, Arlington/VA, 1991), pp. 240-53.
14. E. Van Driest, "Convective Heat Transfer in Gases," in *High-Speed Aerodynamics and Jet Propulsion* (Princeton U. Press, Princeton/NJ, 1959), vol. 5.
15. M. Sibulkin, "Heat Transfer near the Forward Stagnation Point of a Body of Revolution," *Journal of the Aeronautical Sciences*, vol. 19 (1952), pp. 570-1.
16. R. Roberts, "Laminar and Turbulent Flow of Gases," in *American Institute of Physics Handbook* (McGraw-Hill Book Co., New York/NY, 1972), chap. 2u.
17. J. Kestin and R. DiPippo, "Viscosity of Gases," in *American Institute of Physics Handbook* (McGraw-Hill Book Co., New York/NY, 1972), chap. 2r.
18. C. Klein, "Aerodynamic Heating of Hemispherical Irdomes at Supersonic Speeds," *AIAA/ASME Thermophysics and Heat Transfer Conference* (Boston/MA, 16jul74),